

WL-TM-97-3060

**TAILLESS AIRCRAFT CONTROL
ALLOCATION**



James M. Buffington
Control Analysis Section
Flight Dynamics Directorate
Wright Laboratories
Air Force Materiel Command
Wright-Patterson Air Force Base, Ohio 45433-7652

May 1997

FINAL REPORT FOR PERIOD 1 MAY 1997 - 31 MAY 1997

Approved for public release; distribution unlimited

DTIC QUALITY INSPECTED 3

**FLIGHT DYNAMICS DIRECTORATE
WRIGHT LABORATORY
AIR FORCE MATERIEL COMMAND
WPAFB OH 45433-7562**

19970804 032

Tailless Aircraft Control Allocation*

James M. Buffington

Aerospace Engineer, USAF Wright Laboratory

Member, AIAA

Abstract

This paper presents a flight controller for a tailless aircraft with a large suite of conventional and unconventional control effectors. The controller structure is modular to take advantages of individual technologies from the areas of plant parameter estimation, control allocation, and robust feedback control. Linear models generated off-line provide plant parameter estimates for control. Dynamic inversion control provides direct satisfaction of flying qualities requirements in the presence of uncertainties. The focus of this paper, however, is control allocation. Control allocation is posed as constrained parameter optimization to minimize an objective that is a function of the control surface deflections. The control law is decomposed into a sequence of prioritized partitions, and additional optimization variables scale the control partitions to provide optimal command limiting which prevent actuator saturation. Analysis shows that appropriate prioritization of dynamic inversion control laws provides graceful command and loop response degradation for unachievable commands. Preliminary simulation results show that command variable response remains decoupled for unachievable commands while other command limiting methods may result in unacceptable coupled response.

1 Introduction

The next generation United States Air Force fighter aircraft will more than likely have a reduced vertical tail or no vertical tail at all. Radar cross section and structural weight reduction benefits have influenced these tailless aircraft configurations [1]. Tailless configurations, however, present an interesting challenge from a stability and control perspective [2]. Vertical tails provide directional stability and contain the rudder which is typically the primary directional control effector. Lack of a ver-

tical tail undoubtedly relaxes directional stability and reduces directional control power. Advanced fighter configurations may also have relaxed longitudinal stability for reduced supersonic trim drag and enhanced maneuverability which further challenges the flight control system. Unconventional control effectors that provide multi-axis forces and moments may be added to overcome control power deficiencies [3, 1]. The unconventional control effectors must be allocated with other conventional effectors to maintain performance of current fighters. Flight control algorithms must augment the relaxed stability of these configurations and manage the distribution of many control effectors. Flight control technology must therefore pave the way for successful tailless aircraft programs.

A modular control structure for flight control of a tailless aircraft configuration is developed to exploit technological advances in feedback control, parameter estimation and control allocation. The flight controller consists of feedback and feedforward augmentation, control allocation, and parameter estimation modules. The parameter estimation module provides stability and control derivative estimates to the control allocation and augmentation modules. The augmentation module provides flight condition adaptation, desired flying qualities, and robustness to uncertainties. The control allocation module allocates the redundant limited control effectors to optimize an objective, achieve maximum control power, and limit pilot commands to reduce the risk of departure.

The modular flight control structure has been initially applied to a tailless fighter configuration [3]. The flight controller included an inner equalization/outer robust loop augmentation module, an off-line generated database plant estimation module, and simple ganging control allocation module that provided no command limiting. The flight control design was successfully demonstrated for flight of a tailless aircraft configuration with minimal uncon-

*This paper is declared a work of the U.S. Government and is not subject to copyright protection in the United States.

ventional control effectors in a limited envelope.

This paper presents extensions of past work [3] by applying the modular control structure to flight control of a tailless fighter with a larger effector suite than previous work. The most significant extension to past work, however, is to explore the full control allocation capability of the tailless fighter aircraft. Optimal objective control allocation and prioritized control command limiting are formulated as a constrained parameter optimization problem. An objective function of the control deflections is constructed, and achievable commands are realized with control deflections that minimize the objective. Unachievable commands are limited and unstable axes prioritized by decomposing the control law into a prioritized sequence of commands. Scalar multipliers from the parameter optimization solution indicate whether the command is achievable or not and provide scalings for the sequence of commands that provide optimal command limiting and axes prioritization.

2 Model of Aircraft with Redundant Effectors

The aircraft nonlinear equations of motion are well documented [4, 5] and can be represented by a system of ordinary differential equations of the following form

$$\dot{x}(t) = f(x(t), u(t)) \quad (1)$$

where $x \in \mathbb{R}^{n_x}$ is the state and $u \in \mathbb{R}^m$ is the control. At some arbitrary time along an arbitrary trajectory, the aircraft dynamics are approximated by the following set of time-varying differential equations

$$\dot{x}(t) = A(t)x(t) + B(t)u(t) + b(t) \quad (2)$$

where $A(t)$ are the stability derivatives, $B(t)$ are the control derivatives, and $b(t)$ is a bias that includes higher order terms and accelerations due to non-equilibrium or off-trim conditions. These equations are nonlinear in time and non-homogeneous due to the bias.

A set of commanded variables $y \in \mathbb{R}^{n_y}$ is defined by the user as a linear function of the state

$$y(t) = C_y(t)x(t) \quad (3)$$

$$\text{rank}(C_y(t)) = n_y.$$

Note that eq.(3) is nonlinear in time. As shown in [6], the following non-unique state transformation

exists

$$\begin{bmatrix} z(t) \\ y(t) \end{bmatrix} = \begin{bmatrix} C_z(t) \\ C_y(t) \end{bmatrix} x(t) \quad (4)$$

such that $\begin{bmatrix} C_z(t) \\ C_y(t) \end{bmatrix}^{-1}$ exists.

$z \in \mathbb{R}^{n_z} \equiv n_x - n_y$

which transforms the system defined by eqs.(2) and (3) into the following convenient form

$$\begin{bmatrix} \dot{z}(t) \\ \dot{y}(t) \end{bmatrix} = \begin{bmatrix} A_{zz}(t) & A_{zy}(t) \\ A_{yz}(t) & A_{yy}(t) \end{bmatrix} \begin{bmatrix} z(t) \\ y(t) \end{bmatrix} + \begin{bmatrix} B_z(t) \\ B_y(t) \end{bmatrix} u(t) + \begin{bmatrix} b_z(t) \\ b_y(t) \end{bmatrix} \quad (5)$$

Also shown in [6], the control dimension may be reduced for design by introducing a control allocation function ρ if the system in eq.(5) is redundant

$$B_y(t)\rho(d_y(t)) = d_y(t) \quad (6)$$

$$\begin{bmatrix} \dot{z}(t) \\ \dot{y}(t) \end{bmatrix} = \begin{bmatrix} A_{zz}(t) & A_{zy}(t) \\ A_{yz}(t) & A_{yy}(t) \end{bmatrix} \begin{bmatrix} z(t) \\ y(t) \end{bmatrix} + \begin{bmatrix} B_z(t)\rho(d_y(t)) \\ d_y(t) \end{bmatrix} + \begin{bmatrix} b_z(t) \\ b_y(t) \end{bmatrix}$$

$$d_y(t) \equiv B_y(t)u(t)$$

where control redundancy is defined by the following conditions

$$\begin{aligned} \text{rank}(b_{y_i}) &= 1 \quad \forall i = 1, \dots, m \\ \text{rank}(B_y) &= n_y \\ m &> n_y \\ B_y &\equiv [b_{y_1} \quad \dots \quad b_{y_m}] \end{aligned} \quad (7)$$

The square system in eq.(6) provides the design model for the flight controller given in the following section.

3 Controller Structure

The proposed flight controller for the aircraft model in section 2 has a modular structure that benefits from independent technology advances in feedback control, control allocation and plant parameter estimation. The controller structure is given in Fig. 1. The Feedback and Feedforward Augmentation (FFA) module inverts the output dynamics and commands appropriate dynamics to provide desired stability and flying qualities properties in a manner

that is robust to uncertainties. The Control Allocation (CA) module provides actuator commands that optimize an objective, utilize maximum control authority, and limit unachievable commands. The plant MODEL module provides stability and control derivative estimates of the AirCRAFT (A/C) to the FFA and CA modules.

3.1 Plant Model

Currently, off-line generated linear models are used to supply aircraft stability and control derivatives to the augmentation and control allocation modules. The nonlinear aircraft model moments are balanced for wings-level flight at a given Mach number, altitude, and angle-of-attack to establish a nominal flight condition. Perturbational techniques are then used to generate a linear model of the aircraft dynamics near the nominal flight condition of the following form which is identical to the model in eq.(2) at some fixed time

$$\dot{x}(t) = Ax(t) + Bu(t) + b. \quad (8)$$

Note the bias term b that results due to untrimmed forces.

3.2 Feedback and Feedforward Augmentation

Dynamic inversion and proportional/integral compensation is used for robust feedback stability augmentation, and feedforward compensation is used for command augmentation [7, 6]. Dynamic inversion inverts the output dynamics and proportional/integral feedback generates a desired robust loop shape. Proportional gains are used in the feedforward path to obtain desirable flying qualities.

Derivation of the control law begins with the plant model in eq.(6). Recall that this model is square since the number of controls d_y equals the number of outputs y . The dynamic inversion control law is given by [6]

$$d_y^{des} = -A_{yy}z(t) - A_{yy}y(t) - b_y + v. \quad (9)$$

Additional control is accomplished through input v . The following proportional-plus-integral control with feedforward elements around the integrators has been shown [7, 6] to provide satisfactory robustness and flying qualities for fighter aircraft

$$\begin{aligned} v &= \omega_c x_i - \omega_c y + \omega_c f_c y^{cmd} \\ \dot{x}_i &= -\omega_c^2 f_i y + \omega_c^2 f_i y^{cmd}. \end{aligned} \quad (10)$$

The feedforward gain is f_c , and the proportional and integral gains are functions of ω_c and f_i . The closed loop system is given by

$$\begin{aligned} \begin{bmatrix} \dot{z} \\ \dot{y} \\ \dot{x}_i \end{bmatrix} &= \begin{bmatrix} A_{zz} & A_{zy} & 0 \\ 0 & -\omega_c I_{n_y} & \omega_c I_{n_y} \\ 0 & -\omega_c^2 f_i I_{n_y} & 0 \end{bmatrix} \begin{bmatrix} z \\ y \\ x_i \end{bmatrix} \\ &+ \begin{bmatrix} 0 \\ \omega_c f_c I_{n_y} \\ \omega_c^2 f_i I_{n_y} \end{bmatrix} y^{cmd} + \begin{bmatrix} f_z(z, y, x_i, y^{cmd}) \\ 0 \\ 0 \end{bmatrix} \\ &\equiv A_{cl}x_{cl} + B_{cl}y^{cmd}. \\ f_z(z, y, x_i, y^{cmd}) &\equiv B_z \rho(d_y^{des}). \end{aligned} \quad (11)$$

Note that if B_z is sufficiently small [6], then the system in eq.(11) is approximately linear. Further for $B_z = 0$, examination of the characteristic equation zeros may be considered for nominal stability analysis

$$\det(\lambda I_{n_z+2n_y} - A_{cl}) = \quad (12)$$

$$\det(\lambda I_{n_z} - A_{zz})(\lambda^2 + \omega_c \lambda + \omega_c^2 f_i)^{n_y} = 0.$$

So if $\det(\lambda I_{n_z} - A_{zz})$ has no zeros in the right half of the complex plane, nominal stability is insured with a proper choice of ω_c and f_i .

The command/output channels are decoupled due to the noninteracting property of the dynamic inversion control, and the individual channel transfer functions are given by the following

$$\frac{y_j}{y_j^{cmd}} = \frac{\omega_c f_c s + \omega_c^2 f_i}{s^2 + \omega_c s + \omega_c^2 f_i}. \quad (13)$$

where $j = 1, \dots, n_y$. The command channel response is therefore directly related to the control parameters. So nominal stability and performance are readily satisfied with a proportional-plus-integral control structure. However, the proportional and integral feedback gains must also account for system uncertainties. Loopshaping [6] provides a simple procedure for choosing robust feedback gains since the noninteracting property of the dynamic inversion decouples the MIMO aircraft.

3.3 Control Allocation

It is assumed that the control law in eqs.(9) and (10) provides desired loop and command response properties, however the reduced dimension controls

(d_y^{des}) must be resolved into actual control effector commands. The control allocation function in eq.(6) provides the mapping from reduced dimension controls to actual control commands $u = \rho(d_y^{des})$.

The control allocation problem has been stated many times in various forms [8, 6, 9]. The unlimited control allocation problem originates from the control dimension reduction in eq.(6). The unlimited control allocation problem, expressed analytically, is to find a function ρ such that $B_y \rho(d_y^{des}) = d_y^{des}$ for all d_y^{des} . For redundant control effector suites, there are many functions that solve the control allocation problem. The effector redundancy may be exploited to satisfy additional objectives such as minimal radar cross section, drag, or wing loads. However, since there are limits on the control effectors, not all d_y^{des} are achievable. Therefore, d_y^{des} may need to be clipped or limited such that $u = \rho(d_y^{des})$ does not violate actuator limits. Past control allocation research includes algorithms that minimize control deflections [6] or drag [9] and limit unachievable commands by preserving the direction of the original command [10, 11]. However, it is shown later that preserving the direction of the command may undesirably degrade flying qualities.

The following control allocation algorithm provides redundant actuator commands that optimize any objective that is a function of the control deflections. The algorithm also utilizes all of the available control power and limits unachievable commands optimally.

3.3.1 Optimal Objective Control Allocation

Limits on the controls complicate the analytical formulation of the control allocation problem. The unlimited control allocation problem can alternatively be cast into the following linear algebra problem. Find a control u such that $B_y u = d_y^{des}$ for a given d_y^{des} . To exploit redundant effector suites, the following constrained parameter optimization problem is cast from the linear algebra formulation

$$\min J = f(u) \text{ subject to } B_y u = d_y^{des} \quad (14)$$

Further constraints may be added to account for limits on u

$$\begin{aligned} \min J &= f(u) - \epsilon \\ \text{subject to } &\begin{cases} B_y u = \epsilon d_y^{des} \\ 0 \leq \epsilon \leq 1 \\ u_i \leq u_i \leq u_{u_i} : i = 1, \dots, m. \end{cases} \end{aligned} \quad (15)$$

The scalar ϵ allows the algorithm to relax the equality constraint if d_y^{des} is not achievable and therefore provides indication whether d_y^{des} is achievable. If $\epsilon = 1$ then d_y^{des} is achievable, otherwise it is not. In effect ϵ limits d_y^{des} , if necessary, by reducing its magnitude and maintaining its direction. So this optimization formulation could give the same results as some past control allocation work [10, 11]. A more general control allocation framework is desirable to provide greater flexibility in command limiting. Prioritized control leads to this general framework.

3.3.2 Prioritized Control Command Limiting

Recall the control law is in terms of a desired reduced dimension control d_y^{des} . Consider decomposing the control law into a set of partitions

$$d_y^{des} = d_1 + d_2 + \dots + d_k \quad (16)$$

where it is assumed desirable to limit d_y^{des} , if necessary, by first limiting d_k , then d_{k-1} , and so on. This suggests a priority among the control law partitions. Note the partitions and the priority among partitions may not be easy to determine for all control laws. A possible priority for a dynamic inversion control law is developed in a later section, but for now assume the partitions and the priority are given. The following constrained optimization problem ensures the priority

$$\min_{u, \lambda} J = f(u) - \sum_{j=1}^k \lambda_j \quad (17)$$

subject to

$$B_y u = \lambda_1 d_1 + \lambda_2 d_2 + \dots + \lambda_k d_k$$

$$u_i \leq u_i \leq u_{u_i}$$

$$0 \leq \lambda_j \leq 1$$

$$\text{If } \lambda_j = 1 : \lambda_{j-1} = \lambda_{j-2} = \dots = 1$$

$$\text{If } \lambda_j = 0 : \lambda_{j+1} = \lambda_{j+2} = \dots = 0$$

$$\text{If } 0 < \lambda_j < 1 : \begin{cases} \lambda_{j-1} = \lambda_{j-2} = \dots = 1 \\ \lambda_{j+1} = \lambda_{j+2} = \dots = 0 \end{cases}$$

$$i = 1, \dots, m$$

$$j = 1, \dots, k.$$

Prioritized Dynamic Inversion Consider the dynamic inversion control law with proportional-plus-integral compensation in eqs.(9) and (10). The

structure of this control law lends itself to the following control partitions

$$\begin{aligned} d_y^{des} &= d_d + d_p + d_i + d_c \quad (18) \\ d_d &\equiv -A_{yz}z - b_y - A_{yy}y + A_dy \\ A_d &\equiv \text{diag}(A_{yy11}, A_{yy22}, \dots, A_{yy_n, n_y}) \\ d_p &\equiv -A_dy - \omega_c y \\ d_i &\equiv \omega_c x_i \\ d_c &\equiv \omega_c f_c y^{cmd} \end{aligned}$$

where A_{yyjj} is the (j, j) element of A_{yy} . The command part (d_c) provides aggressive command response augmentation. The integral part (d_i) provides desired loop robustness and some command response augmentation. The proportional part (d_p) provides stability augmentation. The cascading and decoupling part (d_d) provides stability and decoupled response. If aggressive reference commands are the main cause of unachievable d_y^{des} , then it seems reasonable to limit d_c before d_i . Since basic stability is accomplished by d_d , then d_d should be the last part that is limited. Stability augmentation is accomplished by d_d and d_p , while command augmentation is accomplished by d_c and d_i . Since stability augmentation is most critical, the following priority is proposed

$$d_y^{des} = \lambda_1 d_d + \lambda_2 d_p + \lambda_3 d_i + \lambda_4 d_c. \quad (19)$$

Whereas some command limiting approaches only reduce feedforward gains, the proposed control priority also reduces loop gains so that pilot commands still affect the aircraft response.

The command and loop responses are analyzed to verify the proposed priority. In each output channel, the command response is given by

$$\frac{y}{y^{cmd}} = \frac{\lambda_4 \omega_c f_c s + \lambda_3 \omega_c^2 f_i}{s^2 + \omega_c s + \lambda_3 \omega_c^2 f_i} \quad (20)$$

and the loop response is

$$L = \lambda_2 \frac{\omega_c}{s} + \lambda_3 \frac{\omega_c^2 f_i}{s^2}. \quad (21)$$

It is seen in Fig.(2) that the loop response gracefully degrades as λ_3 goes from one to zero followed by further graceful degradation as λ_2 goes from one to zero. Similarly, the command response gracefully degrades in Fig.(3) as λ_4 goes from one to zero followed by further graceful degradation as λ_3 goes from one to zero.

3.3.3 Axes Prioritization

Since d_y^{des} is a vector, further priority may be enforced between its elements which provides axes prioritization capability. For brevity, this feature will be demonstrated without partitioning d_y^{des} . However, axes prioritization capability may be applied to each d_y^{des} partition to provide the most general solution. Assume without loss of generality that d_y^{des} has three elements, and it is desired to limit the second element first, the third element second and the first element last. The following scaling matrix will limit d_y^{des} , if necessary, according to the stated axes priority

$$\Lambda = \text{diag}(\lambda_1, \lambda_3, \lambda_2). \quad (22)$$

The following parameter optimization problem is now formulated to account for axes prioritization

$$\min_{u, \lambda} J = f(u) - \sum_{j=1}^3 \lambda_j \quad (23)$$

subject to

$$B_y u = \Lambda d_y^{des}$$

$$u_i \leq u_i \leq u_{u_i}$$

$$0 \leq \lambda_j \leq 1$$

$$\text{If } \lambda_j = 1 : \lambda_{j-1} = \lambda_{j-2} = \dots = 1$$

$$\text{If } \lambda_j = 0 : \lambda_{j+1} = \lambda_{j+2} = \dots = 0$$

$$\text{If } 0 < \lambda_j < 1 : \begin{cases} \lambda_{j-1} = \lambda_{j-2} = \dots = 1 \\ \lambda_{j+1} = \lambda_{j+2} = \dots = 0 \end{cases}$$

$$i = 1, \dots, m$$

$$j = 1, \dots, 3.$$

To combine prioritized control with axes prioritization, a diagonal matrix (Λ_k) must be constructed for each control partition (d_k) to reflect the prioritization between elements of that partition.

3.3.4 Implementation Considerations

Issues primarily related to computational limits become critical for on-line implementation of control allocation algorithms. If the control law is to be digitally implemented, control limits may include actuator position limits, rate limits multiplied by the digital flight control system sample time, and any other limits that may be discretized. The values in the optimization problem of eq.(17) should become increments from current values

$$\begin{aligned} u &= u_0 + u_\Delta \\ d_y^{des} &= d_0 + d_\Delta \end{aligned} \quad (24)$$

where $()_{\Delta}$ indicates increments and $()_0$ current values. For sufficiently fast control update rates, the optimization objective function may be reasonably approximated by a linear function

$$f(u_0 + u_{\Delta}) \approx C_o^T(u_0 + u_{\Delta}) \quad (25)$$

which may reduce computational requirements of the control allocation optimization. However, the linear approximation forces boundary solutions which may result in chattering.

Control Preference Knowledge of a control preference and adaptive linear objective coefficients may assist in the elimination of chattering. Assume a control preference (u_p) that does not violate actuator deflection limits, such as minimum drag or minimum wing root bending moment deflection, is given. In general, the control preference does not achieve the desired y -derivative, i.e. $B_y u_p \neq d_y^{des}$. The solution to the following optimization problem

$$\begin{aligned} \min J &= \frac{1}{2}(u - u_p)^T W_p (u - u_p) \quad (26) \\ \text{subject to } B_y u &= d_0 \end{aligned}$$

always achieves the current y -derivative d_0 and is given by

$$u_{opt} = u_p + W_p^{-1} B_y^T (B_y W_p^{-1} B_y^T)^{-1} (d_0 - B_y u_p). \quad (27)$$

The control u_{opt} is "near" u_p in the sense of the optimization problem in eq.(26), and the weight W_p may be adjusted to guarantee that u_{opt} will not violate actuator deflection limits. The linear objective coefficients in eq.(25) are chosen to always drive the controls toward u_{opt} . Once a control effector is within a tolerance of its optimum defined by the rate limit and control sample rate, it may effectively be removed from the optimization by adjusting its coefficient to zero

$$C_{oi} = \begin{cases} 0 & : |u_{opt,i} - u_{0,i}| \leq u_{r,i} \Delta t \\ -(u_{opt,i} - u_{0,i}) & : \text{else} \end{cases} \quad (28)$$

where u_r is a vector of rate limits.

Sequential Optimization Since the constraints for λ are piece-wise linear in eq.(17), a sequential approach to the optimization may reduce computational requirements. The idea is that a sequence of k optimizations with linear constraints and a single λ element is solved instead of a single optimization with nonlinear constraints and k elements in λ .

The constraints are linear for each sequential optimization, and the number of variables is reduced by $k - 1$. The following optimization problem is solved initially for $q = k$

$$\begin{aligned} \min_{u_{\Delta}, \lambda} J &= f(u_{\Delta}) - \lambda \quad (29) \\ \text{subject to} \\ B_y u_{\Delta} &= \sum_{j=1}^{q-1} d_{\Delta,j} + \lambda d_{\Delta,q} \\ u_{\Delta,i} &\leq u_{\Delta,i} \leq u_{u,i} \\ 0 &\leq \lambda \leq 1 \\ i &= 1, \dots, m. \end{aligned}$$

If there is no feasible solution, solve with $q = k - 1$ and so on. The solution $u_{\Delta} = 0, \lambda = 0$ is always feasible since the current control satisfies $d_0 = B_y u_0$. So, there is always a feasible solution in this sequence if control increments (u_{Δ}) are used.

Integrator Windup Dynamic control partitions may experience integrator windup for commands that are unachievable. However, the command limiting scalings (λ) may be used to prevent integrator windup. For example, the dynamic inversion integral control partition (d_i) in eq.(19) will continue to grow due to the x_i dynamics in eq.(10). Integrator windup is prevented by stopping the integral action and holding x_i constant while $\lambda_3 < 1$.

4 Tailless Fighter Control Allocation

This section describes application of optimal objective control allocation to a tailless fighter aircraft. The tailless aircraft is a 65 deg. sweep delta wing, single engine, multi-role supersonic fighter with internal weapons carriage. A high-fidelity six degrees-of-freedom nonlinear simulation was developed from aerodynamic wind-tunnel data of a scale model generated under the Innovative Control Effectors (ICE) program [3, 1]. The ICE configuration includes a large suite of conventional and innovative control effectors that provide forces and moments in multiple axes. The conventional effectors include elevons, pitch flaps, thrust vectoring, and outboard leading edge flaps. The innovative or unconventional control effectors include spoiler-slot deflectors and all-moving tips.

A dynamic inversion control system for subsonic flight has been developed previously for an ICE configuration without flaps and spoiler-slot deflectors [3]. The past work includes simple ganging control allocation, and the current work develops a more

sophisticated control allocation method for the ICE configuration with the full control effector suite.

The following linear model is generated at Mach 0.4 and 15,000 ft. altitude for demonstration of the optimal objective control allocation

$$\begin{bmatrix} \dot{\alpha} \\ \dot{\beta} \\ \dot{P} \\ \dot{Q} \\ \dot{R} \end{bmatrix} = \begin{bmatrix} -0.6344 & 0.0027 & 0 & 0.9871 & 0 \\ 0 & -0.0038 & 0.1540 & 0 & -0.9876 \\ 0 & -8.2125 & -0.7849 & 0 & 0.1171 \\ -0.5971 & 0 & 0 & -0.5099 & 0 \\ 0 & -0.8887 & -0.0299 & 0 & -0.0156 \end{bmatrix} \begin{bmatrix} \alpha \\ \beta \\ P \\ Q \\ R \end{bmatrix} \quad (30)$$

$$+ \begin{bmatrix} -0.0459 & -0.0459 & -0.0395 & -0.0133 & -0.0133 \\ -0.0047 & 0.0047 & 0 & 0.0031 & -0.0031 \\ 3.7830 & -3.7830 & 0 & 1.8255 & -1.8255 \\ -2.5114 & -2.5115 & -1.9042 & -0.9494 & -0.9494 \\ 0.0453 & -0.0453 & 0 & -0.2081 & 0.2081 \end{bmatrix} \begin{bmatrix} \delta_{e_l} \\ \delta_{e_r} \\ \delta_{p/lap} \\ \delta_{amt_l} \\ \delta_{amt_r} \end{bmatrix}$$

$$+ \begin{bmatrix} -0.0109 & 0 & 0.0217 & 0.0217 & 0.0047 & 0.0047 \\ 0 & 0.0110 & 0.0066 & -0.0066 & -0.0021 & 0.0021 \\ 0 & 0.0790 & -2.0956 & 2.0957 & -0.3067 & 0.3067 \\ -1.1329 & 0 & 1.5046 & 1.5046 & -0.0003 & -0.0004 \\ 0 & -0.8038 & -0.0283 & 0.0283 & 0.0937 & -0.0937 \end{bmatrix} \begin{bmatrix} \delta_{ptv} \\ \delta_{ytw} \\ \delta_{ssd_l} \\ \delta_{ssd_r} \\ \delta_{oblfl_l} \\ \delta_{oblfl_r} \end{bmatrix}$$

Note that this model is of the form in eq.(8) without the bias since it is an equilibrium or trim condition. The control law in eqs.(9) and (10) is completely specified by the uncommanded variables (z), commanded variables (y), and design parameters (ω_c , f_i , and f_c). The commanded variables are chosen based on flying qualities requirements [12] to be stability axis roll rate, pitch rate, and a blend of sideslip and stability axis yaw rate. The uncommanded variables are defined to be angle-of-attack and sideslip which guarantee existence of the transformation inverse in eq.(4)

$$z = \begin{bmatrix} \alpha \\ \beta \end{bmatrix} \quad (31)$$

$$y = \begin{bmatrix} P \cos \alpha_0 + R \sin \alpha_0 \\ Q \\ K_\beta \beta - P \sin \alpha_0 + R \cos \alpha_0 \end{bmatrix}$$

$$K_\beta \equiv -1.$$

The following feedback and feedforward gains are chosen based upon uncertainty bounds and flying qualities requirements for similar fighter aircraft [6]

$$\omega_c = 5 \frac{\text{rad}}{\text{sec}} \quad (32)$$

$$f_i = .25$$

$$f_c = .5.$$

The linear model of the aircraft is considered with actuator position and rate limits to demonstrate the optimal objective control allocation and prioritized control concepts. The control allocation optimization objective is to force the controls toward a zero control preference ($u_p = 0$), i.e. minimum control deflection. This is accomplished using control increments and linear objective coefficients shown in section 3.3.4. Although the algorithm is capable of more complex objective functions, computational requirements may increase significantly for complex objectives. This may be important for the ultimate goal of on-line implementation.

The sequential linear program in eq.(29) is solved for the linear tailless fighter aircraft model to provide minimum drag control allocation for achievable commands and prioritized command limiting for unachievable commands. Note that there are eleven control surfaces so $m = 11$. The dynamic inversion control priority is indicated by the following controller partitions

$$d_1 = d_d \quad d_2 = d_p \quad d_3 = d_i \quad d_4 = d_c \quad (33)$$

The upper and lower control limits are defined by the most restrictive of position limit (lp, up) or product of rate limit (ur) and time step (Δt)

$$\begin{aligned} u_{l,i} &\equiv \max\{lp_i - u_{0,i}, -ur_i\Delta t\} \\ u_{u,i} &\equiv \min\{up_i - u_{0,i}, ur_i\Delta t\} \end{aligned} \quad (34)$$

where $u_{0,i}$ is the i^{th} element of the current control u_0 . The sequential linear program is solved at each simulation time step for the following analysis.

4.1 Simulation Analysis

Simulation responses to simultaneous step commands in roll (y_1) and pitch (y_2) are presented in this section to show the benefits of the prioritized control command limiting. A step pitch command at 1 sec. is followed by a step roll command at 3 sec. for two cases. The first case, indicated in Figs.(4) and (5) by *prior*, is optimal objective control allocation with prioritized control command limiting (see eq.(17)). The second case, indicated in Figs.(4) and (5) by *dir*, is optimal objective control allocation with command limiting that maintains command direction (see eq.(15)). The command variable responses are shown in Fig.(4), and the scalings for unachievable commands are shown in Fig.(5). Note that d_y^{des} is unachievable at the onset of the commands as indicated by $\epsilon < 1$ and $\lambda_4 < 1$. Further, note the coupling of the roll response with the pitch and yaw response due to limiting commands to maintain command direction. However, the prioritized control command limiting only limits d_c which maintains the desired decoupled responses. Also, the *dir* case rise time is longer for the roll response. The control responses are available but are not shown due to space limitations.

4.2 Future Plans

Loop stability during command limiting may be guaranteed for certain fixed scalings (λ), but the scalings are generally dynamic. Stability analysis that captures the dynamic nature of the scalings of the prioritized control command limiting is planned. To date, the current algorithms have only been demonstrated on linear airframe models with nonlinear actuators. Future plans include extension of optimal objective control allocation to the ICE tailless fighter nonlinear 6DOF simulation. The nonlinear 6DOF will allow further analysis such as computational requirements, mode transition effects, robust-

ness to unmodelled dynamics and parametric uncertainty, and effects of additional control effector constraints. Efforts to minimize computational requirements of the algorithms have been accomplished, but a comprehensive computational requirements analysis is necessary. Analysis of transients associated with control allocation mode transition, from minimum drag to minimum wing load for example, will be evaluated. Some noise and uncertainty has been injected into the simulations, however thorough robustness analysis is planned. Control effector interactions, hinge moment limit effects, and loads limit effects will be analyzed in the future as well.

Other plans include using a modified sequential least squares identification algorithm [13, 14] to provide stability and control derivatives to the augmentation and control allocation modules in real-time. This will give the control system reconfiguration capability in the event of battle damage or component failure. The reconfiguration aspect of tailless fighter flight control is investigated in the RESTORE program [1]. Control redundancy will no doubt complicate real-time control derivative identification. However, the optimal objective control allocation algorithm may possibly be augmented to assist in the identification of redundant effector control derivatives.

5 Conclusions

Optimal objective control allocation with prioritized control command limiting is developed as a general framework for redundant effector management and optimal command limiting to prevent actuator saturation. The control allocation problem is posed as a constrained optimization problem with added variables for command limiting. Although the algorithm is valid for complex objectives, linear objectives lead to linear programs which may reduce computational requirements. The control allocation algorithm has been successfully demonstrated on a tailless fighter aircraft to minimize a linear approximation of drag. Prioritized dynamic inversion command limiting maintains decoupled axes responses for unachievable commands, while past command limiting strategies show unacceptable axes coupling.

References

- [1] Fulghum, D. A., "Tailless Designs Touted For

New Combat Aircraft," *Aviation Week & Space Technology*, November 11, 1996, McGraw-Hill Companies.

- [2] Bowlus, J. A., D. Multhopp, and S. S. Banda, "Challenges and Opportunities in Tailless Aircraft Stability and Control," *1997 AIAA Guidance, Navigation, and Control Conference*, New Orleans, LA, August 1997, Invited paper.
- [3] Ngo, A. N., W. C. Reigelsperger, S. S. Banda, and J. A. Bessolo, "Multivariable Control Law Design for a Tailless Aircraft," *1996 AIAA Guidance, Navigation, and Control Conference*, San Diego, CA, July 1996, AIAA 96-3866.
- [4] Miele, A., *Flight Mechanics: Theory of Flight Paths, Vol 1*, Addison-Wesley, Reading, MA, 1962.
- [5] McRuer, D., I. Ashkemas, and D. Graham, *Aircraft Dynamics and Automatic Control*, Princeton University Press, Princeton, NJ, 1973.
- [6] Buffington, J. M., "Control Design and Analysis for Systems with Redundant Limited Controls," Ph.D. Thesis, University of Minnesota, 1996.
- [7] Enns, D., D. Bugajski, R. Hendrick, and G. Stein, "Dynamic inversion: an evolving methodology for flight control design," *International Journal of Control* Vol. 59, No. 1, 1994, pp. 71-91.
- [8] Virnig, J. C. and D. S. Bodden, "Multivariable Control Allocation and Control Law Conditioning when Control Effectors Limit," *Proceedings from the 1994 AIAA Guidance, Navigation, and Control Conference*, Scottsdale, AZ, August 1994, pp.572-582.
- [9] Durham, W., J. Bolling, and K. Bordignon, "Minimum Drag Control Allocation," *1996 AIAA Atmospheric Flight Mechanics Conference Proceedings*, San Diego, CA, July 1996, pp.399-407.
- [10] Adams, R. J., J. M. Buffington, and S. S. Banda, "Design of Nonlinear Control Laws for High Angle-of-Attack Flight," *Journal of Guidance, Control, and Dynamics*, Vol.17, No.4, 1994, pp. 737-746.
- [11] Durham, W. C., "Constrained Control Allocation: Three-Moment Problem," *Journal of Guidance, Control, and Dynamics*, Vol.17, No.2, 1994, pp. 330-336.
- [12] Honeywell Technology Center, "Application of Multivariable Control Theory to Aircraft Control Laws, Final Report: Multivariable Control Design Guidelines," WL-TR-96-3099, May 1996.
- [13] Ward, D. G., R. L. Barron, M. P. Carley, and T. J. Curtis, "Real-time parameter identification for self-designing flight control," *Proc. 46th Annual NAECON*, Dayton, OH, May 1994.
- [14] Chandler, P. R., M. Pachter, and M. Mears, "System Identification for Adaptive and Reconfigurable Control," *Journal of Guidance, Control, and Dynamics*, Vol. 18, No. 3, 1995, pp. 516-524.

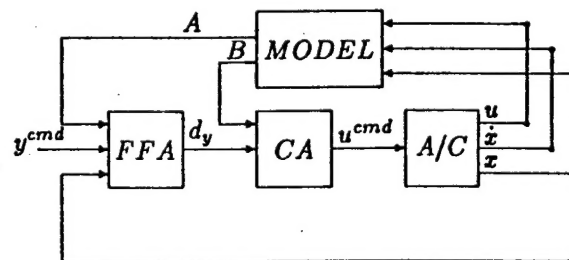


Figure 1: Flight Controller Structure

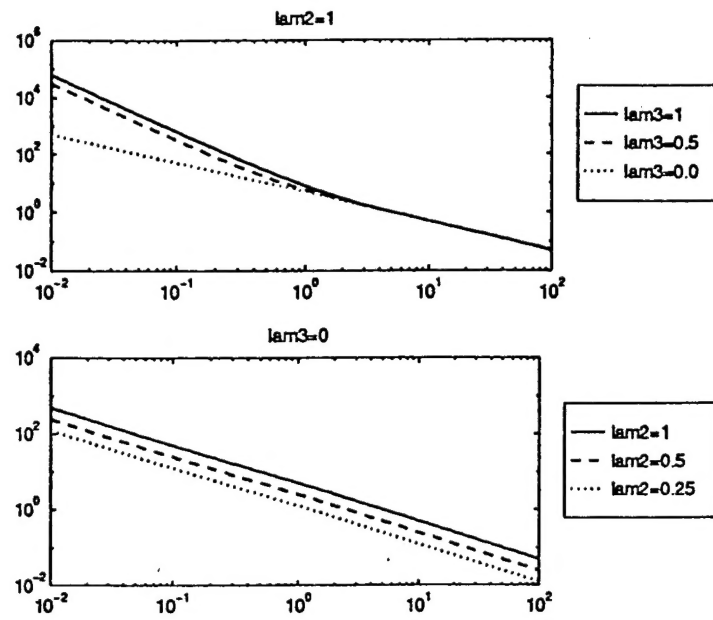


Figure 2: Loop Transfer Response Degradation

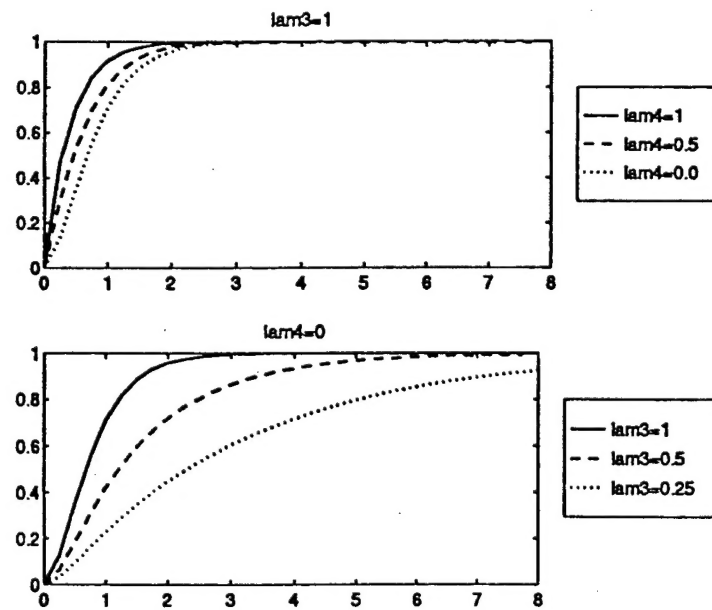


Figure 3: Command Step Response Degradation

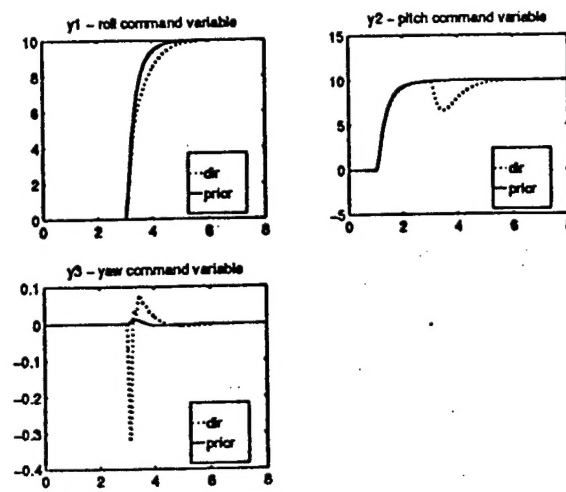


Figure 4: Command Variable Responses

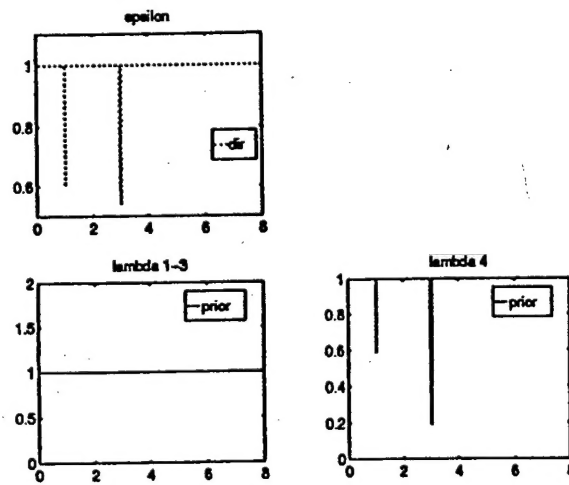


Figure 5: Command Scaling Responses